The Delay/Doppler Radar Altimeter

R. Keith Raney, *Fellow, IEEE*

***Abstract*—The key innovation in the delay/Doppler radar altimeter is delay compensation, analogous to range curvature correction in a burst-mode synthetic aperture radar (SAR). Following delay compensation, height estimates are sorted by Doppler frequency, and integrated in parallel. More equivalent looks are accumulated than in a conventional altimeter. The relatively small along-track footprint size is a constant of the system, typically on the order of 250 m for a Ku-band altimeter. The flat-surface response is an impulse rather than the more familiar step function produced by conventional satellite radar altimeters. The radar equation for the delay/Doppler radar altimeter has an $h^{-5/2}(c\tau)^{1/2}$ dependence on height h and compressed pulse length τ, which is more efficient than the corresponding $h^{-3}c\tau$ factor for a pulse-limited altimeter. The radiometric response obtained by the new approach would be 10 dB stronger than that of the TOPEX/Poseidon altimeter, for example, if the same hardware were used in the delay/Doppler altimeter mode. This new technique leads to a smaller instrument that requires less power, yet performs better than a conventional radar altimeter. The concept represents a new generation of altimeter for earth observation, with particular suitability for coastal ocean regions and polar ice sheets as well as open oceans.**

***Index Terms*—Doppler beam sharpening, radar altimeter, synthetic aperture radar.**

I. Introduction

THE PRINCIPAL objective of a satellite radar altimeter is to measure the height of reflecting facets scanned by passage of the instrument overhead. Geophysical elevation is derived from the record of radar height measurements, corrected with respect to precise orbit knowledge and path delays. Height precision is set by the radar pulse length and by the amount of averaging available for each estimate. Height is defined in the context of this paper as the minimum range between the radar and scatterers that lie along the ground track of the satellite.

By definition, a conventional satellite altimeter [Fig. 1(a) and (b)] uses the echo delays from within the pulse-limited footprint to estimate minimum radar range [8]. Outside of the pulse-limited footprint, each scatterer's echo appears at relatively greater delay. The (compressed) pulse length determines the diameter of the pulse-limited footprint associated with a quasiflat surface [2]. For a typical radar altimeter, such as GEOSAT, the pulse-limited footprint is on the order of 2 km in diameter [6], expanding to many kilometers as large-scale surface roughness increases.

Manuscript received April 1, 1997; revised October 27, 1997.

The author is with The Johns Hopkins University Applied Physics Laboratory, Laurel, MD 20723-6099 USA (e-mail: keith.raney@jhuapl.edu).

Publisher Item Identifier S 0196-2892(98)04976-6.

Pulse-limited operation necessarily implies that conventional altimeters are relatively wasteful of radiated power. For example, the footprint diameter of GEOSAT over a quasiflat surface is less than 1/10 of the antenna pattern within the half-power width. Hence, most of the radiated power falls outside of the pulse-limited area and cannot be used for height estimation. Other disadvantages of conventional radar altimeters include footprint dilation over rougher terrain, and the tendency of the footprint location to hop from one elevated region to another rather than to trace out the elevation profile without negative influence from the topography. Footprint dilation leads to less than optimal estimation of surface height and roughness.

Doppler beam-sharpened (DBS) altimeters have been proposed as a means of reducing the along-track footprint size of a radar altimeter. The performance of DBS altimeters has proven to be very disappointing. The main reason is that relatively few "looks" are available, virtually eliminating most of the incoherent averaging that is essential to precision altimetric measurements. The Johns Hopkins University Applied Physics Laboratory (JHU/APL) delay/Doppler approach is fundamentally different; there is far more averaging in the delay/Doppler approach than is possible from a DBS altimeter.

The principal objectives of the delay/Doppler altimeter [12], [13] are to operate more efficiently and more effectively. The first objective is met by compensating for systematic range delay errors; thus, the entire (beam-limited) along-track signal history contributes to height measurement rather than only the much smaller pulse-limited area. Stated another way, the delay/Doppler altimeter uses much more of the instrument's radiated energy than does a conventional beam-limited altimeter. The second objective is met by using Doppler selectivity to reduce the width of the postprocessing along-track footprint; this minimizes unwanted terrain dependency of the footprint size and position.

The delay/Doppler altimeter uses pulse compression in the range dimension, just as is customary for incoherent radar altimeters [5]. The range signal is a long linearly frequency modulated (FM) pulse, which is multiplied by a delayed replica FM pulse immediately upon reception, and low-pass filtered. The delay is chosen to match the expected range to the mean reflecting surface, the so-called track point. This "deramp" strategy transforms "range" into a continuous wave (CW) signal whose frequency is proportional to height, relative to the track point [7], [15], [16]. A conventional altimeter and the delay/Doppler altimeter both complete range compression by application of an inverse Fourier transform (IFFT) to convert the CW signals into height. These are summed to produce

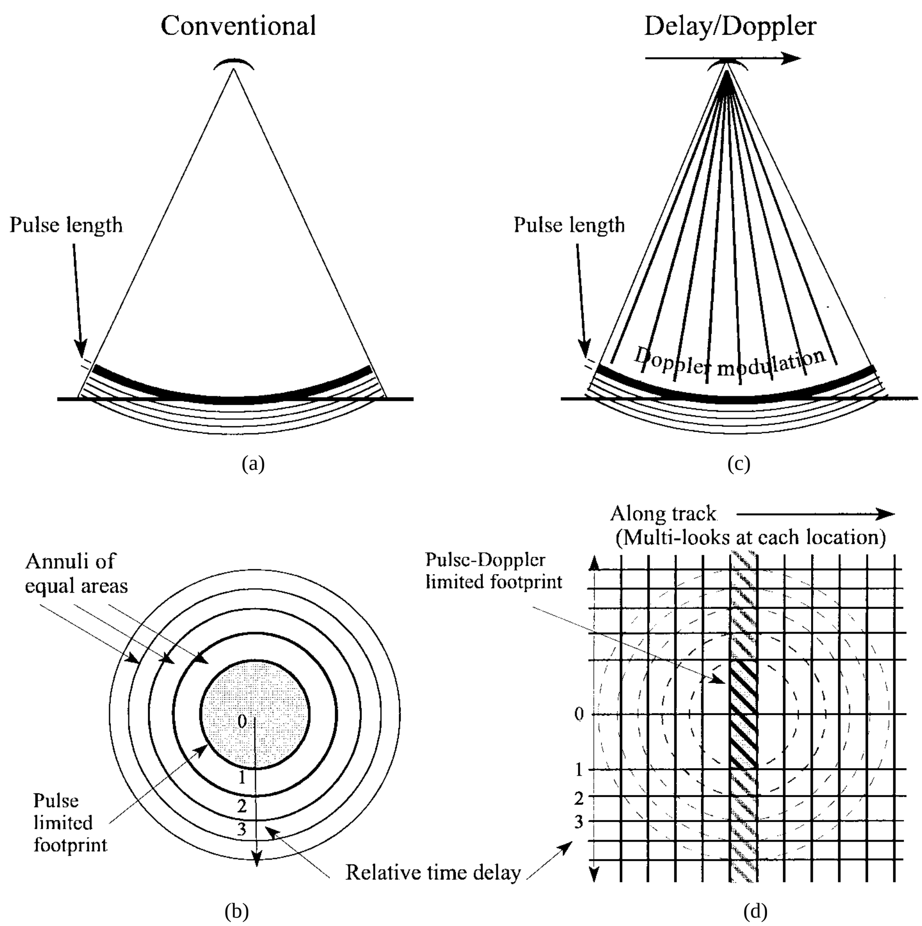

Fig. 1. Comparison of a conventional pulse-limited radar altimeter's (a) illumination geometry side view and (b) footprint plan view, to a delay/Doppler altimeter's (c) illumination geometry side view and (d) footprint plan view. The conventional radar altimeter measurement space is inherently 1-D, whereas that of the delay/Doppler altimeter is 2-D.

the output height waveforms. The compressed pulse length is inversely proportional to the duration of the CW signals.

The delay/Doppler altimeter introduces along-track processing steps after the range deramp and before the range IFFT, the net effect of which is to transform the signal space to two dimensions [Fig. 1(c) and (d)]. The delay/Doppler technique requires coherent correlation within each burst of pulses, in contrast to a conventional altimeter for which pulse-to-pulse correlation is not desirable [16]. The received signals from each burst are stored in memory. A Fourier transform is applied to these data in the along-track dimension, implemented in real time onboard as a set of parallel FFT's that span the range gate width. Signals in the resulting two-dimensional (2-D) range CW/Doppler domain are processed to eliminate the curvature of the range delay. The delay-corrected data are partitioned by Doppler frequency, which is isomorphic to along-track distance from spacecraft nadir. At each Doppler frequency bin, range data are inverse transformed, detected, and accumulated in parallel to form many equivalent looks at that position. As a consequence of the 2-D signal processing unique to the delay/Doppler altimeter, its flat-surface response has an impulse-like shape, in contrast to the step-function response of a conventional radar altimeter (Fig. 2). The JHU/APL has received patent protection on this new concept [12].

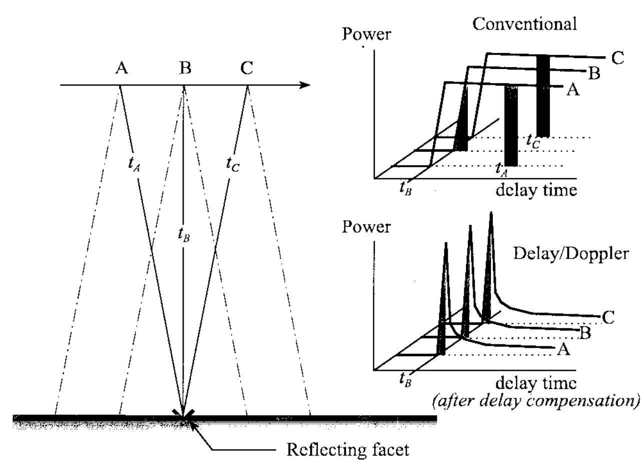

Fig. 2. The round-trip delay time from a scatterer is always longer for all altimeter locations (A, C) that differ from the minimum range position (B), giving rise to the well-known step-function waveform from a conventional altimeter. The delay/Doppler altimeter compensates for the extra delay, from which much sharper waveforms derive.

Although familiar to those versed in synthetic aperture radar (SAR), 2-D coherent signal processing is likely to be a new and perhaps foreign concept to those used to the one-dimensional (1-D) world of conventional radar altimeters. The key ideas are introduced in Sections II and III. Section II describes the

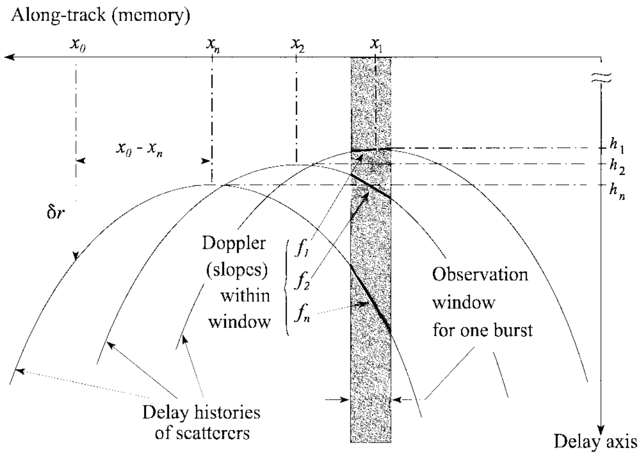

Fig. 3. Each individual range history is hyperbolic, and for a given altitude, its shape is known very well. Delay offset δr can be calculated readily if the scatterer's (along-track) position is known. Unfortunately, the problem is multivalued in the range time/along-track position domain and, hence, admits no unique solution.

objective of range delay compensation. The desired compensation cannot be applied directly, as the range delays in the 2-D signal domain are multivalued. Following the along-track FFT's, however, data in the resulting range (delay)/along-track frequency (Doppler) domain are single-valued, as derived in Section III. Range delay compensation can be applied in this domain. Section IV introduces the new 2-D footprint of the delay/Doppler approach and offers comments on its salient features. Section V describes the flat surface response function of the delay/Doppler altimeter and contrasts it with that from a conventional radar altimeter. Section VI derives the new radar equation applicable to the delay/Doppler altimeter, including its substantial gain advantage when compared to a conventional pulse-limited altimeter. Section VII outlines one method of range gate and pulse timing for a practical spacecraft instrument. The paper closes with comments and conclusions.

II. Delay Compensation

The key to delay/Doppler processing is suggested by the range histories sketched in Fig. 3. The curves describe the relative delay suffered by the signal loci at all points away from minimal radar range. The objective of delay compensation is to eliminate the unwanted extra delay, compared to the minimum range measurement, suffered by the round-trip signal at all other along-track altimeter positions. After compensation, the range indicated for each scatterer over its entire illumination history is equal to its minimum range. The relative delay δr_n for the nth scatterer, given the altimeter along-track position x_0, and the scatterer's along-track position x_n and (minimal) height h_n, is

$$\delta r_n = h_n\left[\sqrt{1+\alpha_R\frac{(x_0-x_n)^2}{h_n^2}}-1\right] \approx \frac{\alpha_R}{2h_2}(x_0-x_n)^2 \quad (1)$$

where the orbital factor α_R is given by

$$\alpha_R \approx \frac{R_E+h_n}{R_E} \approx \frac{V_{S/C}}{V_B} \quad (2)$$

in which R_E is the (local) radius of the earth, h_n is the height (at nadir) of the nth scatterer, V_B is the velocity of the altimeter's antenna illumination along the terrain, and $V_{S/C}$ is the spacecraft orbit velocity. For typical values ($h_n \sim 800$ km, $\alpha_R \sim 1.12$, and $(x_0-x_n) < 8$ km), the extra range delay δr_n goes from zero to about 45 m. Although this may not seem like much, it is large when compared to a typical (compressed) altimeter pulse length of 0.5 m. It is essential that this extra delay be removed if the along-track signal is to be used for precise elevation estimates outside of the pulse-limited zone.

The change in relative delay as a function of range is comparatively small. To prove this, the sensitivity of relative delay to a change in height may be estimated from

$$\frac{\partial \delta r_n}{\partial h_n} = -\frac{\alpha_R(x-x_n)^2}{2}\frac{1}{h_n^2} \Rightarrow$$
$$\partial \delta r_n = -\delta r_n \frac{\partial h_n}{h_n}. \quad (3)$$

Using the same numbers as before, the difference in range delay for a 1-km change in reference height h_n, say from 800 to 801 km, is only 45 $\times$ 1/800 < 6 cm. In similar fashion, it may be shown that the change in relative delay due to the orbital factor α_R is much less than 1 mm. It follows that an acceptable range delay estimate can be derived with only an approximate knowledge of the scatterer's height, and this value may be held constant over the width of the range gate and over the duration of the azimuth signal.

Delay compensation implies that the extra delay is removed from the signal over its history. Given that this unwanted delay is known, and that the signal locus is known, the extra delay could be compensated completely by subtracting an equivalent amount from the indicated range at all points on the along-track range history. This would lead to the range locus having a constant effective height h_n at all observation opportunities.

Unfortunately, it is not possible to apply the delay compensation scheme directly to the received data because to do so would require knowledge of the along-track position x_n of each scatterer. Even more frustrating, the signal loci from more than one scatterer are present in each echo ensemble. Echoes are received simultaneously from all individual scatterers within the illuminated beam width of the antenna, which spans the observation space of the system. Three representative range histories are shown in Fig. 3. Clearly, at any position in the data field, the delay compensation problem is multiple valued, for which a single delay compensation is impossible in the range/along-track domain.

III. Delay/Doppler Domain

Transformation from the along-track signal domain to the along-track frequency (Doppler) domain reduces delay compensation to a single-valued problem. Recall that the *Fourier shift theorem* [17] states that application of a Fourier transform $\mathcal{F}$ to a function with position shift leads to the Fourier transform of the function, multiplied by a CW phase term whose frequency is proportional to the shift. Let the along-track signal history for each scatterer be $a(x)$. Let x_0 be the nadir position of the altimeter and x_n be the along-track

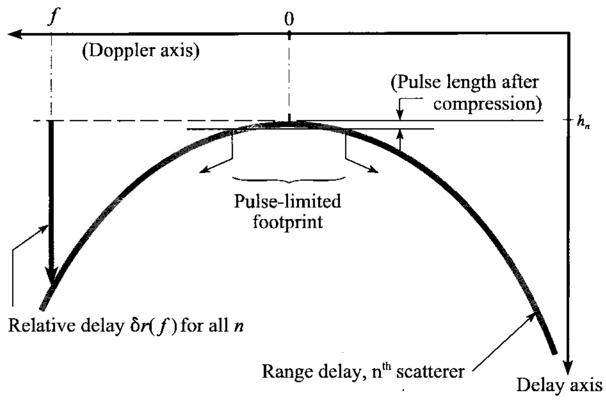

Fig. 4. In the delay/Doppler domain, the relative delay $\delta r(f)$ is a known function of Doppler frequency. Hence, the problem is single valued; relative delay can be eliminated from all signals simultaneously.

position of the nth scatterer. Then the Fourier transform $A(f)$, taken with respect to position x_0 for the nth scatterer, is

$$\mathcal{F}\lfloor a(x - x_n + x_0)\rfloor = A(f)\exp\{-j2\pi f(x_n - x_0)\} \quad (4)$$

where f is (Doppler) frequency in the along-track direction. Thus, an along-track Fourier transform over the ensemble of signal histories in memory yields a unified set of signal range loci (Fig. 4) for which the along-track position of all scatterers relative to spacecraft nadir (zero Doppler) has been relegated to CW phase terms, the ensemble of which constitutes the Doppler spectrum of the transformed signals.

The Doppler spectrum has a geometric interpretation. Doppler frequency is a measure of the slope of the signal (range) history, which has a known functional form. Hence, slope knowledge is equivalent to (along-track) angular offset knowledge, which may be inverted to evaluate the corresponding extra range delay. The angle θ_n at time t between the radar and a scatterer at location t_n along track is one-to-one equivalent to the Doppler shift imposed on the signal. The Doppler is given by the dot product of the viewing unit vector and the velocity vector

$$f = \frac{2}{\lambda}\frac{\vec{r}(t - t_n)\cdot\vec{V}}{|\vec{r}(t - t_n)|}$$
$$f = \frac{2|\vec{V}|\cos\theta_n}{\lambda}. \quad (5)$$

Within the constraints of the near-vertical small angle geometry of a satellite altimeter, the Doppler scaling factor is approximated very well by

$$f \approx \frac{2V_{S/C}}{\lambda}\frac{x_n - x_0}{h_n}\ \text{[Hz]}. \quad (6)$$

Thus, there is a one-to-one correspondence between the observed Doppler frequency (relative to zero) and an individual scatterer's along-track position x_n (relative to the altimeter's position x_0) at all points along track [10]. This powerful rule serves as the radar altimeter *Doppler equivalence theorem*.

The Fourier shift theorem and the Doppler equivalence theorem may be applied to open new possibilities for radar altimetry. As noted in (6), Doppler frequency is related to along-track data position relative to the subsatellite point.

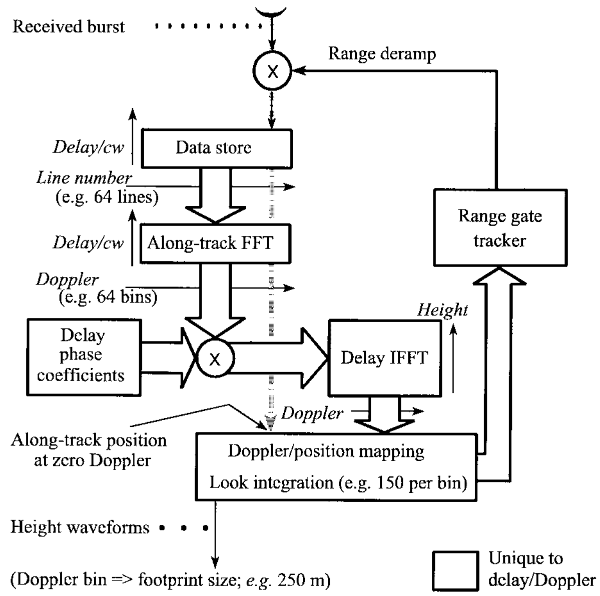

Fig. 5. Logical flow of the delay/Doppler processing scheme. After delay compensation (by application of multiplicative phase shifts) and range IFFT's, data are detected and accumulated by Doppler bin. The process is repeated burst by burst. Each scatterer moves from higher Doppler locations to lower as the altimeter passes overhead.

It follows that the required delay compensation is a known and single-valued function over the delay/Doppler space. The delay increment, in terms of Doppler frequency [14] as its independent variable, is

$$\delta r(f) \approx \alpha_R \frac{\lambda^2 h_n}{8V_{S/C}^2} f^2. \quad (7)$$

Furthermore, such compensation may be applied simultaneously to all echoes included in the Fourier transform. Compensation of this delay could be realized by brute force operations on the data in the range/Doppler domain, using integer shifts and an interpolator. However, there is a better way.

Recall that the deramped data in the range direction appear as constant (CW) frequencies. Each range delay increment translates into an equivalent CW frequency shift. These unwanted frequency shifts may be nullified by multiplying the data field by equal and opposite range CW signals prior to the range IFFT, implementing in effect an inverse Fourier shift operator.

A block diagram of the principal signal processing stages is shown in Fig. 5. The 2-D delay compensation phase multiplier shown in the figure is

$$\Phi(f, t) = \exp\left\{+j2\pi k_R \frac{2}{c}\delta r(f)t\right\} \quad (8)$$

where k_R is the linear FM rate of the transmitted signals. The effect of this phase multiply is to correct the range frequency from each scatterer to CW signals that have the same (range) frequency at all Doppler (along-track) positions at which it is observed. The phase multiply acts on all signals simultaneously.

The data at this stage consist of an ensemble of 2-D CW signals. For each element, frequency in the range direction is proportional to (minimum) delay relative to the range track point, and frequency in the along-track direction is proportional to the scatterer's along-track position relative to the zero-Doppler position.

The remaining data processing is carried out in parallel, consisting of a range IFFT at each Doppler frequency bin, detection, and assignment of the height estimates to their respective along-track positions. The process is repeated over subsequent blocks of data, from which many looks are accumulated at each along-track position. As the altimeter passes over each scatterer, the corresponding height estimates move in sequence from the highest Doppler filter to each lower frequency filter until the scatterer is out of sight. Thus, the final height estimate at each along-track position is the average (incoherent sum, normalized) of estimates from all Doppler filters. If the Doppler filters are designed to span the along-track antenna beamwidth, all data along track contribute to the height estimates. The along-track impulse response is determined by the Doppler filter weightings. Along-track impulse position is determined by the zero-Doppler position for each burst of data.

IV. Footprint

Refer again to the altimeter footprints sketched in Fig. 1. Fig. 1(a) shows the side view of a pulse radiating from a conventional altimeter toward a quasiflat surface. As the pulse propagates, its radially symmetric intersections with the surface define a sequence of spreading annuli as in Fig. 1(b) [8]. It can be shown that the annuli each have equivalent areas, which give rise to a relatively constant backscatter level after the initial response.

As introduced above, the delay/Doppler altimeter [Fig. 1(c)] uses coherent processing over a block of received returns to estimate the Doppler FM imposed on the signals by the forward motion of the altimeter. Doppler analysis of the data allows their relative along-track positions to be estimated relative to the position of the altimeter. It follows that the along-track dimension of the signal data and the cross-track (range or time-delay) dimension are separable. In contrast to the response of a conventional altimeter, which has only one independent variable (time delay), the delay/Doppler altimeter response has two independent variables: along-track position (x) and cross-track position y (functionally related to time-delay t). After delay/Doppler processing, these two variables describe an orthonormal data grid, as shown in Fig. 1(d). With this data space in mind, delay/Doppler processing may be interpreted as an operation that flattens the radiating field in the along-track direction. In this transformed data space, the resolved (x, y) cells have constant along-track length, but their cross-track width decreases as the square root of delay time.

The true nadir point is contained in the plane orthogonal to the satellite ground track for which the Doppler shift is zero. The along-track location of this plane is independent of satellite attitude as well as terrain slope. The delay estimates at all Doppler frequencies can be located along track with respect to nadir. Ideally, the along-track nadir location is equivalent to along-track spacecraft position. Vertical spacecraft velocity will add Doppler shift to the signals, which if not compensated will add unwanted along-track shift to all data positions. To neutralize the effects of vertical velocity, offsetting Doppler shifts can be applied to assure registration of the height estimates accumulated over the sequence of processed bursts that span the along-track length of the antenna illumination pattern.

The along-track velocity ($\sim$6.5 km s^{-1}) of a conventional altimeter causes the effective footprint for a multipulse waveform to be elongated along track. Detected returns from many pulses are averaged together to build each multilook waveform. Such signal summations typically extend over 0.1 s, during which time the antenna illumination pattern progresses in the along-track direction by a distance ($\sim$650 m) that is comparable to the radius of the pulse-limited circle. As a result, the effective footprint for a conventional altimeter, after multilook summation, is a set of elliptical annuli, elongated along track, rather than the circular single-pulse footprints normally cited in the literature. In contrast, multilook processing in the delay/Doppler altimeter does not cause spreading of the along-track footprint. Instead, Doppler signal analysis not only reduces the length of the effective footprint along track, but also synchronizes the relative location of each height estimate with the forward motion of the instrument, thus eliminating along-track elongation of the footprint.

It follows that the customary concept of "flat surface response" applies only to the delay time dimension for a delay/Doppler altimeter. This means that the inherent delay/elevation ambiguity that plagues pulse-limited altimeters is reduced from two spatial dimensions to only one dimension. The cross-track ambiguity that remains is suggested in Fig. 1(d), which shows that at any given Doppler frequency, there are two possible sources for reflections having a given (relative) time delay. These arise from either side of the minimum delay locus, which nominally is the subsatellite track. Of course, the point of first reflection (at zero relative delay time) may be to one side of the subsatellite track, as would be true in general when there is a nonzero cross-track terrain slope. The cross-track ambiguity and the delay/elevation ambiguity both may be at least partially resolved through application of other means, such as the monopulse phase sensing technique [4].

V. Flat Surface Response

The average flat surface response function describes the time-delay history of reflections observed by an altimeter over a quasiflat horizontal surface [2]. (In this work, *quasiflat* means that the observed reflectivity per area increment is independent of incidence over the restricted set of angles illuminated by the radar and there is no perceptible variation in terrain elevation within the illuminated region.) To accommodate the delay/Doppler altimeter, the concept of flat surface response must be extended to two independent variables, one corresponding to relative delay time and one corresponding to the along-track position of the altimeter. The shape of the delay-time response is determined primarily by the resolved scattering area in the cross-track direction. The shape of the corresponding along-track response function is set by weighting in the processor and subject to design optimization.

It is helpful to distinguish between two closely related “flat surface” functions, denoted here as $p_{FS0}(t)$ and $p_{FS}(t)$. The (idealized) flat surface response $p_{FS0}(t)$ was first described by Moore and Williams [8] as the function that accounts for the effects of antenna pattern, illumination geometry, and incoherent surface scattering. The flat surface response $p_{FS}(t)$ includes the physical constraints of the illumination and antenna geometry as well as the impact of (compressed) pulse shape and signal processing. It is this flat surface response that serves as the primary analytical basis for description of the spatial properties of radar altimeters [2], [5].

The difference between these two flat surface functions is subtle, but significant. Recall that the impulse response $p(t)$ describes the output of a (linear) system when its input is an arbitrarily short test signal. Under reasonable conditions, the expected output $g(t)$ from any linear sensor is given by the convolution $g(t) = p(t) * s(t)$ of the sensor's impulse response $p(t)$ over the distribution function $s(t)$ that describes the input data source. It has been shown that the average input data distribution function for a (conventional) radar altimeter is well modeled by a convolution $s(t) = p_{FS0}(t) * q(t)$ of the (idealized) flat surface response $p_{FS0}(t)$ with the topographic distribution $q(t)$ of the reflective points on the surface [2]. The resulting radar altimeter linear model is a triple convolution $g_{alt}(t) = p(t) * p_{FS0}(t) * q(t)$ or (impulse response)∗(idealized flat surface response)∗(topographic distribution) in plain language. This triple convolution may be regrouped as (flat surface response)∗(topographic distribution) or $g_{alt}(t) = p_{FS}(t) * q(t)$, where $p_{FS}(t) = p(t) * p_{FS0}(t)$.

The flat surface (delay time) responses for both a conventional radar altimeter and the delay/Doppler altimeter are shown in Fig. 6. The droop imposed by antenna weighting is also suggested. The underlying analysis assumed that the effective (compressed) radiated pulse was rectangular in both cases. Time delay is shown in units of pulse length. If the effective pulse were weighted, as might be expected in practice, the corners of these response functions would be smoother.

A. Conventional Pulse-Limited Altimeter

The behavior of a conventional satellite radar altimeter [Fig. 6(a)] is well known. Its flat surface response function is

$$\begin{aligned} P_{conv}(t) &= 0, && \frac{1}{\tau}\left[t - \frac{2h}{c}\right] \le 0 \\ &= \frac{t}{\tau}, && 0 < \frac{1}{\tau}\left[t - \frac{2h}{c}\right] \le 1 \\ &= 1, && 1 < \frac{1}{\tau}\left[t - \frac{2h}{c}\right] \end{aligned} \tag{9}$$

where τ is the effective pulse length, h is the altitude, and c is the speed of light. After an initial rise, the response remains constant, more-or-less, subject primarily to decreases from off-boresight antenna pattern weighting. (Of course, antenna pointing errors, or nonzero slope of the illuminated surface, cause departures from this norm [2].) The portion of the flat surface response function that corresponds to the area illuminated by the pulse during the second pulse delay interval is shaded in the figure. The defining characteristic of this response function is that the curve is essentially a step function: once attained, the maximum value is supported for many delay intervals. This is because the areas of the concentric annuli defined by the radiating (compressed) pulse are constant with time.

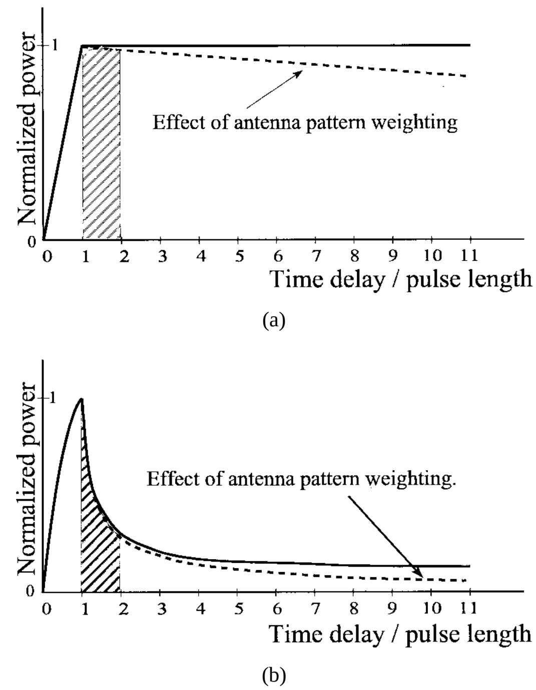

Fig. 6. Typical quasiflat surface response waveforms from (a) conventional satellite pulse-limited radar altimeter and (b) delay/Doppler altimeter. (Note that the power scales are normalized to unity.)

B. Delay/Doppler Altimeter

The delay time response (after processing) of the delay/Doppler altimeter is shown in Fig. 6(b) and has the functional form

$$\begin{aligned} f_{DD}(t) &= 0, && \frac{1}{\tau}\left[t - \frac{2h}{c}\right] \le 0 \\ &= \sqrt{\frac{t}{\tau}}, && 0 < \frac{1}{\tau}\left[t - \frac{2h}{c}\right] \le 1 \\ &= \sqrt{\frac{t}{\tau}} - \sqrt{\frac{t}{\tau} - 1}, && 1 < \frac{1}{\tau}\left[t - \frac{2h}{c}\right]. \end{aligned} \tag{10}$$

This curve represents the (average) strength of the altimeter's response to illumination of a quasiflat surface as a function of time delay, just as in the previous case. As before, the second delay interval is more darkly shaded in the figure. Note that the response to a flat surface for all regions in the second delay zone and beyond have much less relative power for the delay/Doppler altimeter than for the conventional radar altimeter. This is because the area contributing to the response signal decreases as the square root of time.

VI. Radiometric Response

The delay/Doppler altimeter uses signal data from the entire length of the antenna illumination pattern in the along-track direction to estimate the height of each resolved patch of subsatellite terrain. This implies that substantially more integration is possible than in a pulse-limited altimeter. Under the assumption that the dominant scattering mechanism is nonspecular, the integration gain is linear in power. It follows that the total power arising from each resolved cell is *larger* for the delay/Doppler altimeter than for a conventional pulse-limited altimeter, even though the postprocessing footprint size is *smaller*.

A. Conventional Altimeter Radar Equation

The classical radar equation [9], including the range time-bandwidth product (TBP), may be written

$$P_R = \frac{P_T G^2(\theta)\lambda^2(\mathrm{TBP})\sigma}{(4\pi)^3 h^4} \tag{11}$$

where σ is the effective radar cross section of the resolved terrain patch. In the literature of altimetry [7], [8], the radar cross section usually is interpreted to mean

$$\sigma = \sigma^0 A_\sigma \tag{12}$$

where σ^0 is the normalized scattering coefficient of the terrain (dimensionless) and A_σ is the area of the resolved footprint. When the altimeter is pulse-limited, the radius r_{PL} of the limiting circle for the quasiflat surface response function on a spherical earth may be derived from (1) to be

$$r_{PL} = \sqrt{c\tau h/\alpha_R}. \tag{13}$$

The area of the footprint for the pulse-limited altimeter is

$$A_{PL} = \pi r_{PL}^2 = \frac{\pi c\tau h}{\alpha_R}. \tag{14}$$

Thus, the effective received power for a pulse-limited altimeter is

$$P_{PL} = \frac{P_T G^2 \lambda^2 (\mathrm{TBP})\pi c\tau\sigma^0}{(4\pi)^3 h^3 \alpha_R}. \tag{15}$$

B. Delay/Doppler Radar Equation

The same approach may be extended to cover the case of a delay/Doppler altimeter. Its distinguishing feature is delay compensation, after which all reflections from a given scattering area have the same radar range at each and every point in the accumulated signal history. As a consequence, height estimation for each resolved scattering cell benefits from integration as long as that cell is illuminated by the antenna pattern. The delay/Doppler radar equation can be developed in a manner that is similar to well-known results in SAR. For each scattering cell, the equivalent along-orbit integration length L_A is proportional to the length βh of the antenna footprint (Fig. 7), expanded [11] by the orbital factor α_R (2). Here β is the equivalent rectangle width of the antenna along-track power pattern. The along-orbit integration may be interpreted in terms of an equivalent along-track area A_{DD} that contributes to the received signal power for a delay/Doppler altimeter on a single-pulse basis. The cross-track dimension is set by the pulse-limited condition. Thus

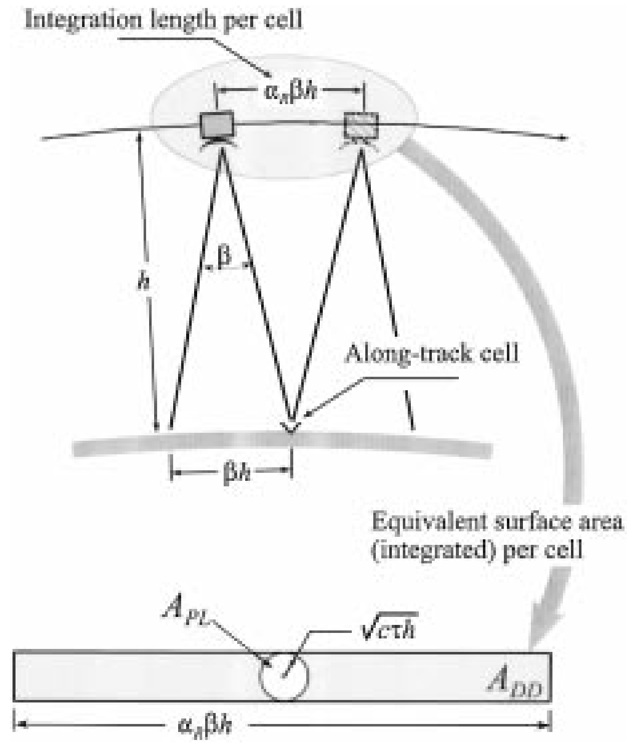

Fig. 7. Area A_{PL} that contributes to the single-pulse height measurement for a conventional altimeter is purely beam-limited. For the delay/Doppler altimeter, the equivalent area A_{DD} that contributes to the integrated power from each resolved cell is pulse-limited across track and its along-track length is determined by the arc length along the orbit from which each resolved cell is illuminated.

$$A_{DD} = 2\alpha_R r_{PL} L_A = 2h\beta\sqrt{c\tau h\alpha_R}. \tag{16}$$

The corresponding integrated received power for the delay/Doppler altimeter is

$$P_{DD}\frac{P_T G^2(\theta)\lambda^2(\mathrm{TBP})\sigma^0}{(4\pi)^3 h^{5/2}} 2\beta\sqrt{c\tau\alpha_R} \tag{17}$$

which has an $h^{-5/2}$ altitude (range) dependence.

At one level, this result should be expected. At least with respect to the altitude dependence, it is the geometric mean between the pulse-limited case (h^{-3}) and the beam-limited case (h^{-2}) derived by Moore and Williams [8]. Furthermore, integration along track for orbital systems always benefits from the ratio of the orbital path to the footprint path radii. Beyond these, however, the result shows another effect that is subtle but may be helpful in system optimization: reduced sensitivity to compressed pulse length τ.

The relative power efficiency of the two altimeters is given by the ratio

$$\frac{P_{DD}}{P_{PL}} = \frac{A_{DD}}{A_{PL}} \tag{18}$$

in which it is assumed that all other factors (such as average transmitted power and antenna gain) are equal in the two cases. To first order, the relative radiometric advantage of

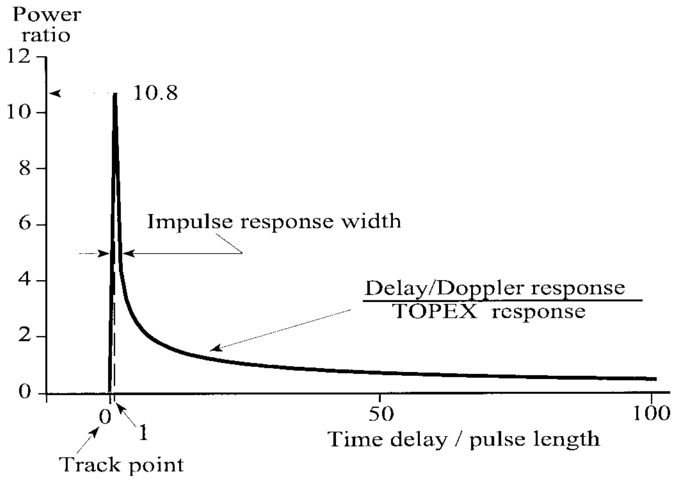

Fig. 8. Given comparable hardware (the same average transmitted power, the same antenna gains, etc.), the response of a delay/Doppler altimeter can be more than 10 dB stronger than the response of a conventional pulse-limited altimeter.

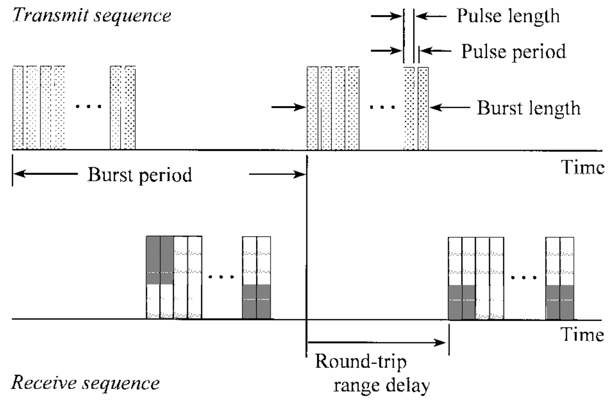

Fig. 9. Timing plan for a burst mode realization of a delay/Doppler altimeter.

the delay/Doppler altimeter over the pulse-limited altimeter is given simply by the ratio of the equivalent areas over which the signals are integrated. It is evident that the delay/Doppler altimeter makes better use of transmitted power, primarily because more of its integration contributes directly to energy at the estimated height of each scatterer.

C. Example

The magnitude of the potential gain improvement can be illustrated through an example. Consider an altimeter that is similar to TOPEX/Poseidon [7] in most regards, having the same average radiated power, same beamwidth, same pulse compression and range resolution, etc. The only difference is that the altimeter is operated in the delay/Doppler mode. The radiometric performance of the delay/Doppler altimeter compared to that of TOPEX/Poseidon is given by the ratio of their two (flat surface) response functions, scaled by their relative powers (18). The result, plotted in Fig. 8, shows that the radiometric response of the delay/Doppler altimeter is more than ten times stronger at the desired altitude mark than the response of a conventional radar altimeter, which is an advantage of more than 10 dB.

VII. Onboard Along-Track Processing

The delay/Doppler altimeter requires pulse-to-pulse signal coherence to support the along-track fast Fourier transform (FFT). Coherence implies that the pulse repetition frequency (PRF) must be higher than that used on previous radar altimeters, such as TOPEX. This section elaborates on consequences of the high PRF requirement and suggests a design approach that leads to a satisfactory solution for the along-track timing and data sequencing issues.

At each of its two frequencies, the TOPEX altimeter [7] uses a burst sequence of 38 pulses. Each pulse has about 100-μs length and 220-μs pulse repetition period (4500-Hz PRF). The burst length corresponds to the round-trip pulse propagation time from the altimeter to the surface. Reflected signals are received during the $\sim$100-μs interval between transmitted pulses. The timing between bursts is controlled so that the receive intervals are synchronized with the arriving echoes. These parameters were chosen to make the best use of the available time, under the constraints of minimizing transmitted peak power and maximizing the number of looks.

The approach described in more detail in the following paragraphs has a superficial similarity to TOPEX, in that the burst length corresponds to the round-trip range delay time. In contrast to the TOPEX model, however, for the delay/Doppler altimeter, the interburst interval is used for echo reception, not the interpulse periods. As will be seen, this supports a robust range gate timing scheme yet maintains an efficient duty cycle. This burst sequence strategy has other features that work well with the delay/Doppler data processing requirements.

The suggested burst mode plan is shown in Fig. 9. Burst length can be constant, chosen to be a little less than the minimum round-trip delay time from the altimeter to the surface. The PRF must be higher than the Doppler bandwidth of the echo ensemble, yet it must be low enough that the pulse length is less than the pulse period (1/PRF). Once chosen, the PRF can be constant. The number of pulses transmitted in each burst can be a constant. The burst period should be variable, but a variation of only 5% would be more than adequate to accommodate the expected span of ranges to be presented to a system onboard a satellite in circular orbit. The burst period is constrained to map the position of all height estimates onto along-track locations that are congruent with those of the previous burst. The processing is completed for each along-track position by summation of the detected height estimates from the entire Doppler spectrum as the altimeter passes over.

A. Design Constraints

This particular burst mode strategy, combined with the desire for pulse-to-pulse coherence, leads to design rules and performance constraints for the delay/Doppler altimeter, which are explored in this section. It turns out that election of the interburst interval as the echo reception window, rather than the interpulse period, constrains the design to a relatively narrow set of options. Fortunately, these options should be acceptable for many applications. There are tradeoffs that are considered further as they arise in the discussion.

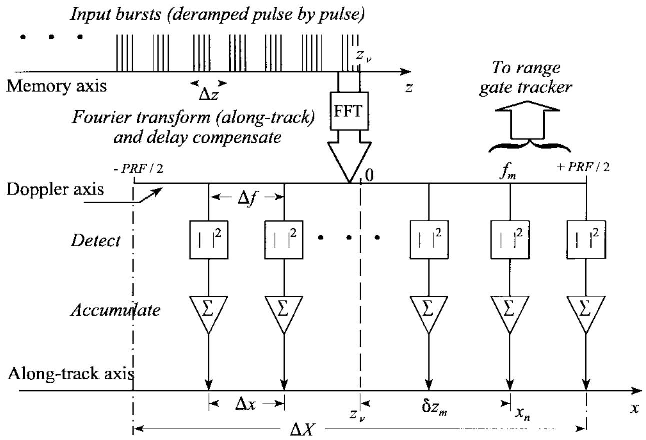

Fig. 10. Along-track processing plan for a delay/Doppler altimeter.

The principal signal sequences are sketched in Fig. 10. Each received pulse echo is deramped in the usual way [7] and recorded into memory. Subsequent operations are carried out burst by burst. The transformations shown are applied in parallel to all data within the range gate. At each range index, the along-track transform integrates over the block of (complex) data in memory after all pulses from each burst are received. Delay compensation is applied at this stage, included by inference in the FFT operator shown in the figure. The resulting frequency distribution is the Doppler domain, constrained to the Nyquist band defined by the PRF. The frequency increments Δf and the corresponding along-track position increments Δx are determined by system and burst parameters. In each Doppler frequency bin, the data are detected and added to sums being accumulated for each along-track position x_n, whose locations are known through the Doppler frequency f_m and the burst location z_ν. The questions to be addressed here relate to the size and location of these various sequences.

B. Timing Within Each Burst

Pulse-to-pulse coherence requires that the on-orbit distance between transmissions should be less than half of the along-track aperture diameter D of the radar antenna. The same limitation follows from the requirement that the Doppler spectrum arising from the antenna pattern should be sampled at or above the Nyquist rate. Thus, the pulse period T_{prf} must satisfy

$$T_{\text{prf}} = \frac{1}{\text{PRF}} \le \frac{D}{2V_{S/C}} \tag{19}$$

where $V_{S/C}$ is the spacecraft velocity along its orbit. The number of pulses per burst N_B is given by the ratio of burst length to pulse period. Burst length τ_B must be less than the round-trip delay time T_R corresponding to the altimeter height h

$$T_R = \frac{2h}{c} \tag{20}$$

where c is the speed of light. Thus, the number of pulses per burst is constrained by

$$N_B = \frac{T_R}{T_{\text{prf}}} > \frac{4hV_{S/C}}{cD}. \tag{21}$$

There is one design choice implicit in this constraint: *antenna size*. An antenna diameter of 1.5 m and an orbit at 800-km altitude leads to the constraint $N_B > 54$. Since the along-track processing strategy is based on an FFT, it makes sense to select N_B to be a power of two, which in this case would be 64. As will be seen below, the burst length may be fine tuned to optimize output sample spacing. For the moment, let $\tau_B = 0.9T_R$. The corresponding burst length would be 4.8 ms, which implies a pulse period $T_{\text{PRF}} = 75$ μs and a PRF $= 13.333$ kHz.

The band of Doppler frequencies that is unambiguously sampled by the PRF is given by ($-$PRF/2 $< f \le$ PRF/2). The along-track FFT leads to N_B discrete frequencies f_m in the frequency (Doppler) domain, with uniform intersample spacing $\Delta f = \text{PRF}/N_B$. Using the numbers derived above, $\Delta f = 208$ Hz. It may be shown that the Doppler frequencies that span one PRF interval correspond to an along-track spread ΔX of scatterers that also are unambiguously sampled [10]. Neglecting the second-order effects of earth rotation

$$\Delta X = \frac{h\lambda}{2V_{S/C}T_{\text{prf}}} \tag{22}$$

where λ is the radar wavelength.

The design question now becomes: what is the size of the along-track cell Δx that corresponds to each resolved Doppler cell Δf? From the above

$$\Delta x = \frac{\Delta X}{N_B} = \left(\frac{c\lambda}{4V_{S/C}}\right)\frac{T_R}{\tau_B} \tag{23}$$

where the enclosed term in effect is a constant of the system. For a given orbital altitude, the velocity parameters are predetermined. Wavelength may be open to designer option, but it is often determined by other criteria. Spacecraft velocity is only weakly dependent on altitude for the low earth orbits of interest to altimetry. The ratio of round-trip delay time to burst length is subject to choice, but it must be larger than unity. Surprisingly, the along-track cell is not dependent on the radar PRF, even though cell size is derived directly from the Doppler spectrum. Thus, for an altimeter that uses interburst echo reception, the Doppler resolved along-track footprint is a constant of the system, independent of orbital altitude, to first order.

Fortunately, the ensuing cell spacing is useful; $\Delta x = 243$ m in the present case. The cell size can be adjusted (within limits) by small changes in the burst length τ_B. In general, a Ku-band delay/Doppler burst mode altimeter in an 800-km orbit would have an along-track cell size of 219 (T_R/τ_B) m.

Let z_ν be the along-track location of the altimeter at the end of the νth burst, at which time the FFT transformation of that data block to the Doppler domain is completed. There is a one-to-one mapping between Doppler frequency f_m and along-track position δz_m relative to the zero Doppler position [as in (6)], such that for $n = \nu + m$, $x_{\nu+m} = z_\nu + \delta z_m$.

Thus, the range history at every Doppler frequency can be assigned to its corresponding along-track position as each block is processed.

The upper bound on pulse length τ_u is set by the PRF according to

$$\tau_u < \frac{1}{\mathrm{PRF}} \tag{24}$$

which for 13.333 kHz is about 75 μs. In the burst mode described here, there is no need for an interpulse period larger than zero. The mode allows the pulses to be concatenated to completely fill the burst length, becoming in effect a sawtooth-modulated CW signal. The PRF also sets an upper limit on the unambiguous range gate length ΔR

$$\Delta R < \frac{cT_{\mathrm{prf}}}{2} = \frac{c}{2\mathrm{PRF}} \tag{25}$$

where for 13.333 kHz is about 11.25 km, which is more than adequate.

C. Timing Between Bursts

For each burst period T_B, the altimeter footprint progresses along its surface track. The along-track burst spacing ΔX_B is given by

$$\Delta X_B = T_B V_{Foot} \tag{26}$$

where V_{Foot} is the velocity of the altimeter footprint along the illuminated track on the surface [10]. The minimum allowable burst period is $2\tau_B$ or about 10 ms for the example under discussion, for which case, $\min \Delta X_B \approx 67$ m. Any larger burst period is admissible, although it is reasonable to adopt the along-track cell dimension Δx as the upper bound. Then

$$2\tau_B < T_B < \frac{\Delta x}{V_{Foot}} \doteq T_f. \tag{27}$$

The N_B data points from each block should be colocated with the corresponding data points from all other blocks, which implies that the burst period T_B must be an integer fraction $1/n$ of the cell period T_f, which for this example is about 35 ms. Furthermore, it is desirable to maximize the number of range samples per cell. Then the optimum burst period T_B and burst periods n per cell may be found from

$$\max n \text{ s.t.} \left\{ 2\tau_B < \frac{1}{n}T_f = T_B \right\}. \tag{28}$$

For the present example, $n = 3$ and $T_B \approx 12$ m. The output positions of all range estimates are indexed along track by one bin after each group of three bursts are processed. This leads to an along-track impulse response that is weighted and has a half-power width of Δx, or about 250 m for this example.

The number of statistically independent looks available at each along-track cell position may be found from the equivalent rectangle width of the antenna pattern and the numbers derived above. Let the antenna beamwidth in the central along-track section be $\beta \approx \lambda/D$. Then the equivalent along-track distance is $L = \alpha_R h\beta$. The number of looks N_L at each cell is

$$N_L = \frac{nL}{\Delta x} = \frac{\alpha_R h\beta}{V_{Foot}T_B} \tag{29}$$

which in the present case is approximately 150 looks at 800-km altitude. This would expand to about 200 looks at the TOPEX altitude of 1334 km. Note that these looks are for each cell whose dwell time is about 35 ms. In order to compare 200 looks to the TOPEX example, the number of looks needs to be increased in proportion to its 53-ms track interval [7]. Thus, 200 $\times$ (53/35) $\approx$ 300, which is larger than the 228 samples that TOPEX averages in an equivalent time period.

D. The Need for Focusing

The foregoing has been predicated on a simple isometry between Doppler frequency and along-track spatial position. This equivalence is valid for an along-track resolution that is comparable to or larger than the first Fresnel zone [1]. In SAR parlance, this zone is known as the unfocused SAR resolution [3]. Using the classic quarter wavelength criterion, it may be shown that the radius a_0 of the first Fresnel zone is

$$a_0 = \sqrt{\frac{h\lambda}{2}} \tag{30}$$

which leads to an along-track (unfocused) dimension of 180 m from an altitude of 800 km (or about 230 m from an altitude of 1334 km). As these quantities are less than the desired along-track cell size of 250 m, the principle of Doppler equivalence can be applied in its simplest form and the along-track processing task is trivial. If a smaller along-track cell size is desired, such as for altimetry over land, or a very high satellite altitude or longer wavelength were chosen, the along-track processor would have to incorporate phase matching to achieve the focusing required.

E. Comments

This section attempts to make two general points. First, the high-level timing and pulse sequencing for a delay/Doppler altimeter can be organized so that useful performance is obtainable without stressing hardware limits, in spite of the rather high PRF requirement. Second, there are several general rules within which a design may be optimized. It is noteworthy that an along-track spatial cell of about 220 m emerges as a canonic number for a Ku-band altimeter. Furthermore, it is satisfying that this number may be achieved with along-track processing that consists primarily of one set of parallel FFT's and associated accumulators.

The burst technique described here uses the quiescent part of the burst period for echo reception. This might be called the *closed burst method*. An alternative approach would be to use the interpulse periods in subsequent bursts for echo reception, as is done by TOPEX. This might be called the *open burst method*. Design constraints for the open burst method differ from those derived here. The open burst method imposes increasingly difficult constraints as the radar PRF is increased. In particular, range gate acquisition and convergence are compromised and the available pulse length and range gate window are decreased considerably, in comparison to the closed burst method. Nevertheless, the open burst method remains a possibility if there is a requirement to sharpen along-track resolution below about 200 m, and the radar wavelength is not a parameter of choice.

VIII. Conclusions

The delay/Doppler altimeter represents a new class of radar altimeter. The onboard algorithm compensates for the along-track component of the incrementally larger range delay suffered by all scatterers when they are not within the beam-limited (minimum range) footprint. Implementation depends on access to the delay/Doppler signal domain. In turn, this implies that the pulse-to-pulse data sequence must be coherent, so that a Fourier transform can be used to expose the along-track (Doppler) frequencies. In this domain, the delay curvatures are known and can be fully compensated by a phase multiply. The technique is analogous to range curvature correction used in SAR processing. Data rates admit real-time implementation with compact onboard hardware.

An example has been worked to show that substantially sharpened along-track resolution can be achieved with a simultaneous increase in the number of looks, at least in comparison with the best available pulse-limited altimeter. Indeed, it can be shown that the number of statistically independent looks per along-track distance is always larger for the delay/Doppler radar than for a conventional radar altimeter. These benefits are a direct consequence of integration over the full along-track beamwidth, a feature unique to the delay/Doppler approach. Direct benefits of the delay/Doppler delay compensation include: 1) increased efficiency of height estimation, 2) increased geometric stability of the height estimation footprint, and 3) increased averaging for each elevation estimate, leading to reduced estimation variance. These technical benefits lead to an ocean altimeter that provides improved performance while requiring fewer onboard resources. Furthermore, the peaked impulse response waveform and the stability of the instrument's footprint should help to extend radar altimetry to more demanding applications, such as polar ice sheets.

Acknowledgment

The author has benefitted from numerous animated discussions with colleagues. The comments, suggestions, and creative questions from R. Jensen have been especially helpful, and they are gratefully acknowledged.

References

[1] P. Beckman and A. Spizzichino, *The Scattering of Electromagnetic Waves from Rough Surfaces.* London, U.K.: Pergamon, 1963.
[2] G. S. Brown, "The average impulse response of a rough surface and its applications," *IEEE Trans. Antennas Propagat.,* vol. AP-25, pp. 67–74, Jan. 1977.
[3] L. J. Cutrona and G. O. Hall, "A comparison of techniques for achieving fine Azimuth resolution," *IRE Trans. Military Electron.,* vol. MIL-6, pp. 119–133, 1962.
[4] J. R. Jensen, "Angle measurement with a phase monopulse radar altimeter," *IEEE Trans. Antennas Propagat.,* to be published.
[5] J. L. MacArthur, C. C. Kilgus, C. A. Twigg, and P. V. K. Brown, "Evolution of the satellite radar altimeter," *Johns Hopkins APL Tech. Dig.,* vol. 10, no. 4, pp. 405–413, 1989.
[6] J. L. MacArthur, P. C. Marth, Jr., and J. G. Wall, "The GEOSAT radar altimeter," *Johns Hopkins APL Tech. Dig.,* vol. 8, no. 2, pp. 176–181, 1987.
[7] P. C. Marth, J. R. Jensen, C. C. Kilgus, J. A. Perschy, J. L. MacArthur, D. W. Hancock, G. S. Hayne, C. L. Purdy, L. C. Rossi, and C. J. Koblinsky, "Prelaunch performance of the NASA altimeter for the TOPEX/Poseidon project," *IEEE Trans. Geosci. Remote Sensing,* vol. 31, pp. 315–332, Mar. 1993.
[8] R. K. Moore and C. S. Williams, Jr., "Radar terrain return at near-vertical incidence," *Proc. IRE,* Feb. 1957, vol. 45, pp. 228–238.
[9] E. M. Purcell, "The radar equation," in *Radar System Engineering,* L. N. Ridenour, Ed. New York: McGraw-Hill, 1947, ch. 2.
[10] R. K. Raney, "Doppler properties of radars in circular orbits," *Int. J. Remote Sensing,* vol. 7, no. 9, 1986, pp. 1153–1162.
[11] ——, "Considerations for SAR image quantification unique to orbital systems," *IEEE Trans. Geosci. Remote Sensing,* vol. 29, pp. 754–760, Sept. 1991.
[12] ——, "Delay compensated Doppler radar altimeter," United States Patent 5 736 957, April 7, 1998 (international patents pending).
[13] ——, "A delay/Doppler radar for ice sheet monitoring," in *Proc., Int. Geosci. Remote Sensing Symp. IGARSS'95,* Florence, Italy, July, 1995, pp. 862–864.
[14] R. K. Raney, H. Runge, R. Bamler, I. G. Cumming, and F. H. Wong, "Precision SAR processing using chirp scaling," *IEEE Trans. Geosci. Remote Sensing,* vol. 32, pp. 786–799, July 1994.
[15] J. L. Walker, "Range-Doppler imaging of rotating objects," *IEEE Trans. Aerosp. Electron. Syst.,* vol. AES-16, pp. 23–52, Jan. 1980.
[16] E. J. Walsh, "Pulse-to-pulse correlation in satellite radar altimeters," *Radio Sci.,* vol. 17, pp. 786–800, July/Aug. 1982.
[17] P. M. Woodward, *Probability and Information Theory, with Applications to Radar.* London, U.K.: Pergamon, 1953.

R. Keith Raney (S'61–M'62–SM'80–F'91) was with the Canada Centre for Remote Sensing, Ottawa, Ont., from 1976 to 1994, where he helped to initiate the Radarsat mission and was responsible for the conceptual design of the SAR system. He contributed to the conceptual design of NASA's Magellan, the European Space Agency's ERS-1 SAR and scatterometer, and the Shuttle Imaging Radar SIR-C. He was scientific authority for the world's first digital processor for satellite SAR data (Seasat, 1978) and contributed to the design of the X-SAR digital processor at DLR, Germany. He is currently a member of the Principal Professional Staff, Space Department, The Johns Hopkins University Applied Physics Laboratory, Laurel, MD, and is the Assistant Supervisor of the Ocean Remote Sensing Group. He is the principal inventor for the United States patent on the chirp scaling SAR processing algorithm and has a patent on the delay/Doppler radar altimeter. These and other contributions in remote-sensing systems, theory, and applications are documented in more than 300 professional publications.

Dr. Raney has been an Associate Editor for the *International Journal of Remote Sensing* since its inception in 1980 and Associate Editor (radar) for the IEEE Transactions on Geoscience and Remote Sensing since 1982. He is a past President of the Geoscience and Remote Sensing Society (1988 and 1989) and a Fellow of the Electromagnetics Academy. He is a recipient of the Outstanding Achievement Award and the Outstanding Service Award of the IEEE Geoscience and Remote Sensing Society, a Group Achievement Award for the Magellan Radar Science Team, as well as other awards.